4

Petrologic Study of Explosive Pyroclastic Eruption Stage in Shirataka Volcano, NE Japan: Synchronized Eruption of Multiple Magma Chambers

Masao Ban[1], Shiho Hirotani[2], Osamu Ishizuka[2] and Naoyoshi Iwata[1]
[1]*Department of Earth and Environmental Sciences, Yamagata University,*
[2]*Geological Survey of Japan/AIST*
Japan

1. Introduction

Some of detailed petrologic studies on rock samples of middle to large sized explosive pyroclastic eruptions recently revealed that the eruptions were caused by simultaneous eruption of multiple distinct magma chambers beneath the volcanoes (e.g., Nakagawa et al. 2003: Shane et al. 2007). It is very important to examine the genetic relationships among the magmas to understand the magma feeding system which caused such explosive eruptions. The explosive pyroclastic eruption stage in Shirataka volcano, NE Japan (Fig. 1) is one of potential candidates for such kind of researches. The aim of this study is to reveal the magma feeding system beneath Shirataka volcano in the explosive pyroclastic eruption stage and examine the genetic relationships among magmas involved in the explosive eruption.

2. Geologic outline of the Shirataka volcano

The northeast Japan arc (Fig. 1) is one of the representative island arcs. The volume distribution of volcanic products, excluding caldera-related felsic rocks, clearly reveals the existence of two volcanic chains: the frontal row (Nasu volcanic zone) and the back arc row (Chokai volcanic zone) (e.g., Kawano et al. 1961; Tatsumi and Eggins 1995). The Shirataka volcano is situated in the back arc row (Chokai volcanic zone) (Fig. 1). The geologic studies of the Shirataka volcanoes have been performed by many researchers (e.g., Mimura & Kanno, 2000; Ishii & Saito, 1997). Based on the results of these studies, the activity of the Shirataka volcano (0.9-0.7 Ma) is summarized to three stages; strato-cone building, explosive pyroclastic eruption, and lava-dome + block-and-ash flow forming stages (Table 1). The Kokuzo lava, the Numata pumice flow deposit, and Hagino block-and-ash flow deposit + four lava domes (Shiratakayama, Kitsunegoe, Nishikuromoriyama lava dome group + Higashikuromoriyama lava dome) were formed in each stage. Subsequently, the Shirataka volcano collapsed, creating a horseshoe-shaped caldera of ca. 4 km diameter (Yagi et al., 2005).

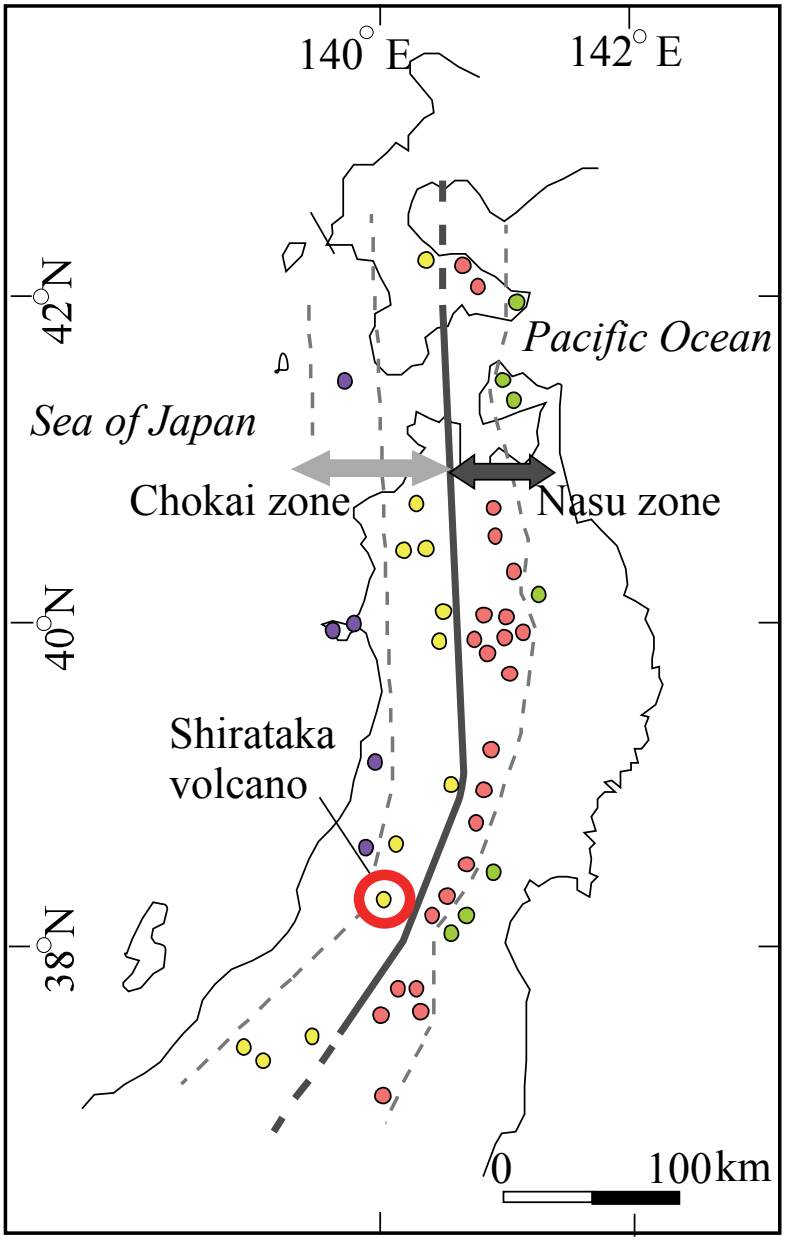

Fig. 1. Location of the Shirataka volcano in the northeast Japan arc. Circles represent Quaternary stratovolcanoes in the northeast Japan arc. The distribution of the volcanoes is from Nakagawa et al. (1988). The distribution of the volcanoes are divided into four volcanic zones: Aoso-Osore (green circle), Sekiryo (orange circle), Moriyoshi (yellow circle), and Chokai (purple circle) zones from trench to rear arc side (Nakagawa et al., 1988).

stage 3: lava-dome & block-and-ash flow forming stage		
Four lava domes*	⇒	medium-K; low-Cr type
Hagino block-and -ash flow deposit	⇒	medium-K; high- & low-Cr types
stage 2: explosive pyroclastic eruption stage		
Numata pumice flow deposit	⇒	medium-K; low-Cr type
stage 1: strato-cone building stage		
Kokuzo lava	⇒	medium-K; high- & low Cr types low-K; high- & low Cr types

Table 1. Simplified stratigraphic relationships and rock series & types of the eruptive products form the Shirataka volcano. *Four lava domes, the Shiratakayama, Kitsunegoe, Nishikuromoriyama lava domes group + Higashikuromoriyama lava dome

3. Petrologic outline of eruptive products from the Shirataka volcano

3.1 Petrography

The eruptive products of the Shirataka volcano are andesitic to dacitic lavas in the first and third stages, but the products are mainly pumice with minor amount of scoria in the second explosive pyroclastic eruption stage. The banded pumice, composed of white pumice and black scoria parts, is rarely observed in the second stage. Mafic magmatic inclusions (~30 cm) are observed in all lavas (Hirotani & Ban, 2006; Hirotani et al., 2009). These are thought to be quenched products of the mafic magma (e.g., Eichelberger, 1980; Bacon, 1986). According to Hirotani & Ban (2006) and Hirotani et al. (2009), the lavas, pumice, and scoria are porphyritic (total phenocryst: ca. 23-40 vol.%) andesitic to dacitic (57.2-65.7 wt% SiO_2), with orthopyroxene, clinopyroxene, plagioclase, and Fe-Ti oxide, with or without hornblende, quartz and olivine phenocrysts. The mafic inclusions are light to dark gray colored, usually rounded in form, and moderately vesiculated, are porphyritic basalt to andesite (48.3-58.5 wt% SiO_2). The total volume of phenocrysts is <ca. 5 vol.% in basalt, and ca. 10 vol.% in basaltic-andesite to andesite, with orthopyroxene, clinopyroxene, and plagioclase, and with or without olivine and quartz phenocrysts. The groundmass has quenched diktytaxitic texture (Bacon, 1986).

3.2 Petrographic evidence for magma mixing and variety of the phenocrysts

The mafic inclusions and disequilibrium phenocryst assemblages (Sakuyama, 1981) such as Mg-rich olivine co-existing with quartz and/or magnesio-hornblende are observed in most of the samples. These features suggest that most of the rocks from Shirataka volcano were formed by magma mixing/mingling (Hirotani & Ban, 2006; Hirotani et al., 2009). Correspondingly, the chemical compositions of phenocrystic minerals show variability. Based on the chemical compositions with textural features, Hirotani & Ban (2006) grouped phenocrystic minerals into several groups. The phenocrysts form different groups cannot co-exist in equilibrium each other by the point of view of their chemical compositions. In the cases

of the stages 1 and 3 products, the groups are named to population I, II, and III by Hirotani et al., (2009). Here we refer "population" as "group". Group I includes An-rich plagioclase, Mg-rich olivine and Mg-rich clinopyroxene. Most of these phenocrysts show compositional normal zoning. Group II includes An-poor plagioclase, Mg-poor orthopyroxene, Mg-poor clinopyroxene, hornblende, quartz, titanomagnetite, and ilmenite. Most of the phenocrysts in this population except for Fe-Ti oxides, show compositional reverse zoning and dissolution textures, such as sieved textures (Tsuchiyama, 1985) or embayed form. Group III is made of smaller phenocrysts of plagioclase, olivine, orthopyroxene, and clinopyroxene. These are interpreted to reflect relict cores from a mafic magma, relict cores from a silicic magma, and minerals growing in the hybrid magma caused by mixing the two magmas precipitated the crystal cores of the groups I and II (Hirotani & Ban 2006).

3.3 Rock series and type of eruptive products of the Shirataka volcano

Hirotani & Ban (2006) presented major and trace elements (Ba, Rb, Sr, Zr, Nb, Y, V, Cr, and Ni) compositional data for the studied samples from all stages of the Shirataka volcano. All samples of the Shirataka volcano plot within calc-alkaline series, and most of them belong to medium-K by the definition of Gill (1981), but the lavas and mafic inclusions from the earlier phase of the cone building stage belong to low-K series (Hirotani and Ban, 2006; Hirotani et al., 2009) (Fig. 2a). All of samples from stage 2 belong to medium-K series, but the pumice has slightly lower K_2O contents than the scoria.

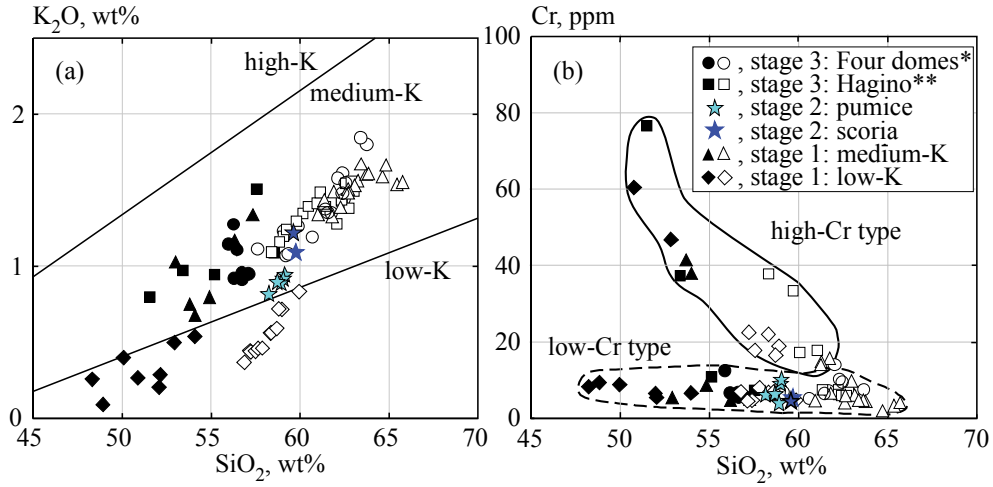

(a) (b)

Fig. 2. K_2O vs. SiO_2 (a), in the left figure Cr vs. SiO_2 (b) in the right figure variation diagrams of the eruptive products from the Shirataka volcano (modified after Hirotani et al., 2009). Data are from Hirotani & Ban (2006). The boundary lines between low-K and medium-K, and medium-K and high-K are from Gill (1981). Filled symbols are mafic inclusions and open ones are host rocks. *Four domes consist of the Shiratakayama, Kitsunegoe, Nishikuromoriyama lava dome group + Higashikuromoriyama lava dome; **Hagino, the Hagino block-and-ash flow deposit

Furthermore, Hirotani et al. (2009) defined the high- and low-Cr types for the rocks from the Shirataka volcano. Cr and Ni contents of the former type are >20 ppm and >5 ppm, 48-55 wt% of SiO_2. Whereas, those of the latter type are ca. 15 ppm and ca. 3 ppm respectively for a given SiO_2 range of 48-55 wt%. Both types are observed in the low and medium-K series. The host lavas having high-Cr type mafic inclusions show higher Cr and Ni contents than those with low-Cr compositions. Consequently these lavas are referred to as high- and low-Cr type lavas, respectively (Fig. 2b). All the samples from stage 2 are low-Cr type.
In addition, the high-Cr rocks always have lower Sr isotope ratio than the low-Cr type rocks for a given range of silica contents of a same geologic or petrologic unit in the cases of stages 1 and 3 (Hirotani et al., 2009). All the samples from stage 2 show similar Sr isotope ratio to the medium-K, low-Cr type rocks in the first stage or those in the early part of the third stage.

4. Uranium, Thorium, and Hafnium contents of the eruptive products from the Shirataka volcano

Hirotani & Ban (2006) and Hirotani et al. (2009) pointed out that the compositions of the samples from the explosive pyroclastic eruption stage show similar features as the medium-K series, low-Cr type rocks of the other stages (Fig. 2), except for the following features. The pumices have extremely higher Zr contents than any other samples from the Shirataka volcano (Fig. 3), and these show slightly lower K_2O contents than the other medium-K lavas from the other stages (Fig. 2a). The higher Zr contents could be attributed to the presence of accessory minerals such as zircon and this would be confirmed by analysing Hf, Th, and U contents. (e.g., Rowe et al. 2007).

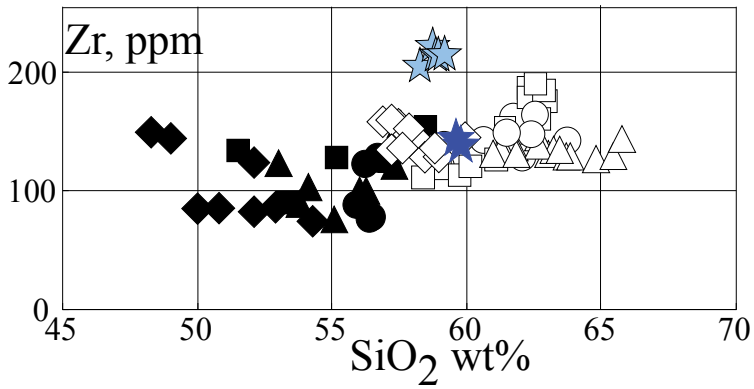

Fig. 3. Zr vs. SiO_2 diagram of the eruptive products from the Shirataka volcano (modified after Hirotani & Ban, 2006). Data are from Hirotani & Ban (2006). Symbols are the same as in Fig. 2.

4.1 Analytical method

Concentrations of Hf, Th and U were determined by ICP-MS on a VG Platform instrument at the Geological Survey of Japan/AIST following the method of Ishizuka et al. (2010). About 100 mg of sample powder was dissolved in a HF-HNO_3 mixture (5:1) using screw-top Teflon beakers on hotplate, followed by fusion with Na_2CO_3 (0.5 g) at 1,050℃. After evaporation to dryness, the residues were re-dissolved in 2% HNO_3 prior to analysis. In and

Re were used as internal standards, while JB2 and JB1a solutions diluted by the same method to the samples were used as external standards during ICP-MS measurements. Instrument calibration was performed using 5-6 solutions made from international rock standard materials. Reproducibility is generally better than ±6% (2 s.d.).

4.2 The analytical results

The representative data are listed in Table 2 and the data are plotted as the SiO_2 variation diagrams in Fig. 4.

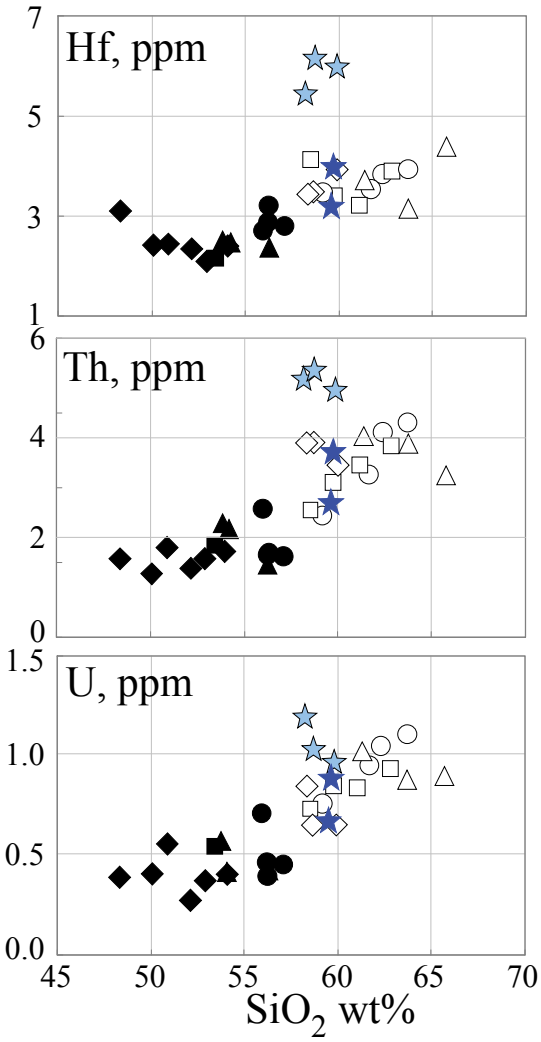

Fig. 4. Hf, Th, and U contents against SiO_2 contents of the samples from the Shirataka volcano. Symbols are the same as in Fig. 2.

stage	1	1	1	1	1	1
series	low-K	low-K	low-K	low-K	low-K	low-K
type	high-Cr	high-Cr	low-Cr	low-Cr	low-Cr	low-Cr
ppm						
Hf	2.12	2.45	3.93	2.36	3.50	2.44
Th	1.52	1.80	3.41	1.37	3.85	1.29
U	0.36	0.54	0.65	0.27	0.64	0.40
stage	1	1	1	1	1	1
series	low-K	low-K	medium-K	medium-K	medium-K	medium-K
type	low-Cr	low-Cr	high-Cr	high-Cr	high-Cr	low-Cr
ppm						
Hf	2.42	3.10	3.67	2.48	2.41	4.37
Th	1.69	1.52	3.95	2.23	2.12	3.15
U	0.40	0.39	1.00	0.56	0.40	0.87
stage	1	1	2 (pumice)	2 (pumice)	2 (pumice)	2 (scoria)
series	medium-K	medium-K	medium-K	medium-K	medium-K	medium-K
type	low-Cr	low-Cr	low-Cr	low-Cr	low-Cr	low-Cr
ppm						
Hf	3.12	2.33	6.16	5.39	5.96	3.23
Th	3.83	1.36	4.91	5.10	5.26	2.71
U	0.86	0.41	0.93	1.18	1.09	0.67
stage	2 (scoria)	3 (Hagino*)	3 (Hagino*)	3 (Hagino*)	3 (Hagino*)	3 (Hagino*)
series	medium-K	medium-K	medium-K	medium-K	medium-K	medium-K
type	low-Cr	high-Cr	high-Cr	high-Cr	low-Cr	low-Cr
ppm						
Hf	4.02	3.22	2.17	3.40	3.90	4.12
Th	3.70	3.41	1.83	3.07	3.82	2.52
U	0.89	0.83	0.54	0.84	0.92	0.72
stage	3 (Domes**)	3 (Domes**)	3 (Domes**)	3 (Domes**)	3 (Domes**)	3 (Domes**)
series	medium-K	medium-K	medium-K	medium-K	medium-K	medium-K
type	low-Cr	low-Cr	low-Cr	low-Cr	low-Cr	low-Cr
ppm						
Hf	3.84	2.90	3.47	2.82	3.93	2.72
Th	4.05	1.63	2.44	1.59	4.25	2.54
U	1.03	0.39	0.75	0.45	1.10	0.70
stage	3 (Domes**)	3 (Domes**)				
series	medium-K	medium-K				
type	low-Cr	low-Cr				
ppm						
Hf	3.54	3.21				
Th	3.23	1.64				
U	0.94	0.45				

Table 2. Hf, Th, and U contents of representative samples from the Shirataka volcano. Hagino*, the Hagino block-and-ash flow deposit; Domes**, the Shiratakayama, Kitsunegoe, Nishikuromoriyama lava dome group + Higashikuromoriyama lava dome

The Hf, Th, and U contents of rocks from stages 1 and 3 are plotted on the same compositional trends in the silica variation diagrams. These contents gradually increase with increasing SiO_2 content (Fig. 4). The ranges of Hf, Th, and U contents of rocks from stages 1 and 3 are 2.1 to 4.4, 1.4 to 4.1, and 0.3 to 1.0, respectively (Table 2). The ranges of Hf, Th, and U contents of scoria samples from stage 2 fall in the ranges of those from stages 1 and 3. However, the pumice samples of stage 2 are plotted in the higher areas than the compositional trends defined by the samples from stages 1 and 3 in the Hf, Th, and U vs. SiO_2 diagrams (Fig. 4). The contents of these elements in the pumice samples are extremely higher than the other ones (Table 2).

5. Discussion

Previous petrologic studies (Hirotani & Ban, 2006; Hirotani et al., 2009) on samples from the first and third stages revealed that (1) all products were formed by magma mixing between mafic and felsic end-member magmas, (2) both end-member magmas changed their compositions with time, (3) the felsic end-member magma was formed by the melt extraction or re-melting of partially or fully crystallized mafic end-member magma of the same activity. The evidence for (1) includes the existence of mafic inclusions in all lava samples, disequilibrium phenocryst assemblages (Sakuyama, 1981) such as Mg-rich olivine and quartz, and wide compositional ranges in plagioclase phenocryst in all samples. The estimated end-member magmas for geologic or petrologic units of stages 1 and 3 are presented in Table 3. As can be observed in the table, the compositions of both the two end-members change temporally.

stage 3: lava-dome & block-and-ash flow forming stage		
Four lava domes*	; medium-K, low-Cr type	; 52.00% SiO_2 and 0.60% K_2O (mafic end-member), 70.00% SiO_2 and 2.20% K_2O (felsic end-member)
Hagino block-and-ash flow deposit	; medium-K, high-Cr type	; 49.50% SiO_2 and 0.64% K_2O (mafic end-member), 66.50% SiO_2 and 1.75% K_2O (felsic end-member)
Hagino block-and-ash flow deposit	; medium-K, low-Cr type	; 50.50% SiO_2 and 0.80% K_2O (mafic end-member), 66.00% SiO_2 and 1.65% K_2O (felsic end-member)
stage 1: strato-cone building stage		
Kokuzo lava	; medium-K, high-Cr type	; 51.00% SiO_2 and 0.50% K_2O (mafic end-member), 66.50% SiO_2 and 1.85% K_2O (felsic end-member)
Kokuzo lava	; medium-K, low-Cr type	; 52.00% SiO_2 and 0.85% K_2O (mafic end-member), 67.50% SiO_2 and 1.70% K_2O (felsic end-member)
Kokuzo lava	; low-K, high-Cr type	; 48.00% SiO_2 and 0.20% K_2O (mafic end-member), 64.50% SiO_2 and 0.85% K_2O (felsic end-member)
Kokuzo lava	; low-K, low-Cr type	; 49.00% SiO_2 and 0.21% K_2O (mafic end-member), 64.00% SiO_2 and 0.75% K_2O (felsic end-member)

Table 3. Temporal change of the mafic and felsic end-members compositions from stages 1 and 3 in the Shirataka volcano. Data are from Hirotani et al. (2009). *Four lava domes, the Shiratakayama, Kitsunegoe, Nishikuromoriyama lava domes group + Higashikuromoriyama lava dome

Similarity of Sr and Nd isotope ratios within the same Cr-type host rocks and mafic inclusions of the same geologic unit shows the consanguinity of the mafic and felsic end-members for each case. The trace element calculations showed that the felsic end-member

cannot be explained by the fractional crystallization process but by the remelting process of the solidified mafic end-member leaving behind gabbroic residue (Hirotani et al., 2009). The genesis of felsic magmas have been explained by similar process in many cases (e.g. Feeley et al, 1998; Hansen et al., 2002, Smith et al., 2006; Vogel et al, 2006; Ban et al., 2007).

The pumice and scoria in the stage 2 possess evidence of mama mixing, such as dissolution textures in plagioclase phenocrysts, disequilibrium phenocryst assemblages, and wide compositional variation in plagioclase phenocrysts. Thus the pumice and scoria could also be formed by magma mixing (Hirotani & Ban, 2006). The compositions of the end-member magmas for the products of stages 1 and 3 have been well discussed (Hirotani et al., 2009), because the compositional ranges of the samples from stages 1 and 3 are wide and thus it was possible to determine the compositions of end-member magmas using the magma mixing lines in the compositional variation diagrams. However, pumice and scoria samples from the stage 2 display very narrow compositional ranges. It was impossible to determine the end-member compositions in these cases using the same method applied for stages 1 and 3 samples. Thus the compositions of the end-member magmas still remain in unknown. In the following sections, we will define these end-member compositions using another method.

5.1 Estimation of the compositions of the end-member magmas for the pumice and scoria in the explosive pyroclastic eruption stage

The juvenile fragments of the explosive pyroclastic eruption stage are mainly pumice with minor amount of scoria, and these also possess petrologic features of mixing of two end-members (Hirotani & Ban, 2006). However there is very little clue to estimate the end-member compositions because of the very narrow compositional ranges of the pumice and the scoria. Thus, here we assume that the end-member compositions of the pumice and scoria are similar to one of the estimated end-member compositions for stages 1 and 3 eruptive products. The chemical compositions of the scoria fall in the ranges of the products of the early part of the third stage (Figs. 2, 3 & 4). Thus the end-member compositions of the scoria would be the same as in the early part of the third stage. On the other hand, the pumice shows higher Zr, Hf, Th, and U contents than any other samples in the Shirataka volcano.

In Fig. 5, we compare the compositions of glass inclusions in pyroxene phenocrysts of pumice to those from stages 1 and 3. Representative compositional data of the glass inclusions are presented in Hirotani & Ban (2006). The compositional range of the glass compositions from pumice is similar to those from the medium-K products of stage 1 in Fig. 5. Therefore, it is reasonable to consider that the felsic end-member compositions of the pumice are also similar to the above mentioned ones. In this case, the mafic end-member compositions should plot on the silica poorer extensions of the mixing lines tying the felsic end-member and pumice compositions (Fig. 6). In this figure, the mafic end-member of the low-K samples of stage 1 is on the extension line (orange colored dotted line in Fig. 6). Here, we assume that the compositions of the mafic end-member are the same as those of low-K products of stage 1. In the next step, we determined the felsic end-member compositions of the pumice, using the tie lines of the assumed mafic end-member and pumice compositions on the SiO_2 variation diagrams, assuming the silica content of the felsic end-member is the same as that of the medium-K products of stage 1. The obtained chemical compositions of the felsic end-member are similar to those of the medium-K products of stage 1, except for higher Zr, Hf, Th, and U contents.

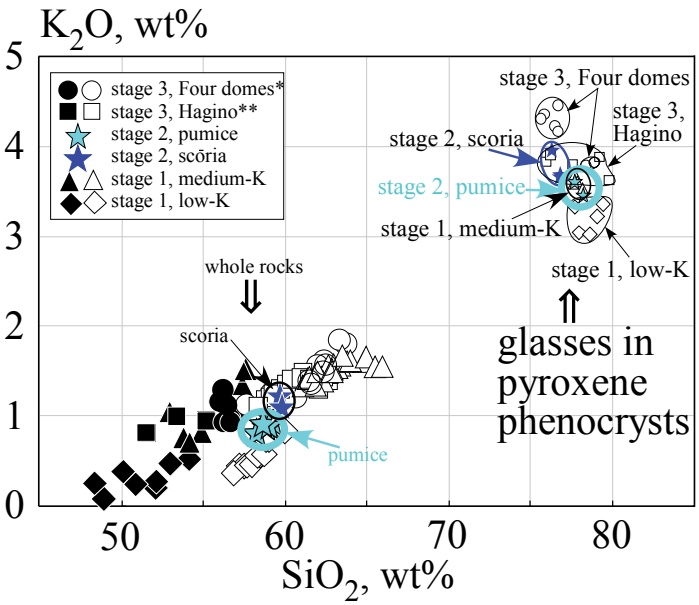

Fig. 5. K_2O-SiO_2 diagram showing the compositions of glass inclusions in pyroxene phenocrysts from each stage in the Shirataka volcano. *Four domes, the Shiratakayama, Kitsunegoe, Nishikuromoriyama lava dome group + Higashikuromoriyama lava dome; **Hagino, the Hagino block-and-ash flow deposit

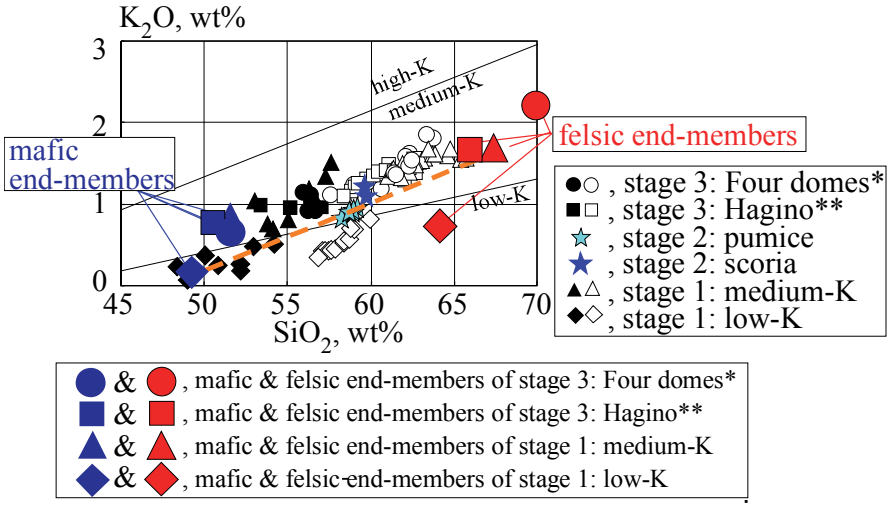

Fig. 6. K_2O-SiO_2 diagram showing the end-member compositions for the pumice and scoria from stage 2 in the Shirataka volcano. The boundary lines of low-K and medium-K, and medium-K and high-K are from Gill (1981). The dotted line shows the mixing line for the pumice. *Four domes, the Shiratakayama, Kitsunegoe, Nishikuromoriyama lava dome group + Higashikuromoriyama lava dome; **Hagino, the Hagino block-and-ash flow deposit

5.2 Melting of accessory zircon with thorite inclusions in producing the felsic end-member magmas for the pumice in stage 3 in the Shirataka volcano

During dormancy between stages 1 and 2, the magma chamber filled with the felsic end-member of the medium-K samples in the first stage would become a mush chamber (e.g., Huber et al., 2010) by the crystallization. In the second stage, new magma injection from deeper levels would re-activate the mushy chamber. This re-activated magma would become to felsic end-member magma for the pumice in the second stage. Such re-activation process of the old magma chambers is thought to be common in producing felsic magmas (e.g., Tamura & Tatsumi, 2002; Girard & Stix, 2009; McCurry & Rodgers, 2009). The higher Zr, Hf, Th, and U contents of the felsic end-member magma can be explained by the melting of the accessory zircon minerals during the re-activation (Wolff et al., 2006). The estimated Zr content of the felsic magma can be obtained by melting of zircon-bearing rock (0.04% of the melt should be from zircon melting). Accordingly, the Hf, Th, and U contents in the zircon are calculated to be ca. 11,500, 10,000, and 1,100 ppm, respectively (Fig. 7). The Hf, Th, and U contents in zircon minerals were reported by many researches (e.g., Rubatto & Hermann, 2007). The calculated Hf content of ca. 11,500 ppm is in the range of reported Hf contents in zircon. On the other hand, the calculated Th and U contents of ca. 10,000 and 1,100 ppm are exceed the ranges of Th and U contents in zircon in equilibrium with the felsic end-member (e.g., Rubatto & Hermann, 2007). Recently, Paquette & Mergoil-Daniel (2009) reported that zircon crystals sometimes include tiny thorite inclusions. The Th and U contents in thorite are much higher than in zircon. Thus, the high Th and U contents can be ascribed to the melting of thorite-bearing components during the re-activation.

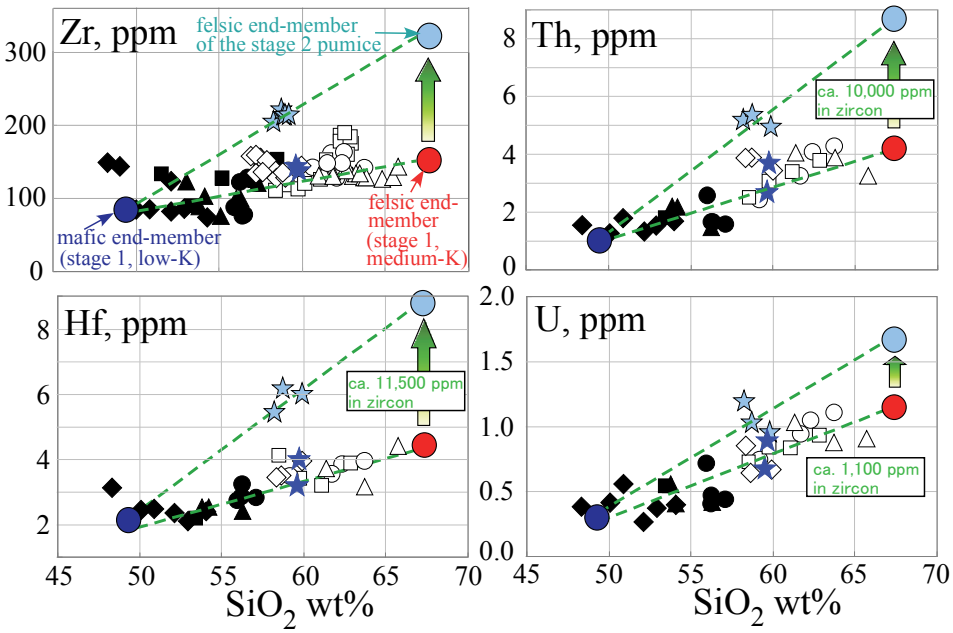

Fig. 7. Plots of Zr, Hf, Th, and U vs. SiO_2 showing the estimated felsic end-member magma compositions for the studied pumice. Symbols, other than the end-members are the same as in Fig. 2.

5.3 The magma feeding system for the explosive pyroclastic eruption stage
5.3.1 Formation of mixed magma for the pumice

As discussed above, the felsic end-member of medium-K samples of the first stage would be re-activated at the second stage and became the felsic end-member magma for the pumice. The end-member magma chamber would be stored in shallower part of the crust. The re-activation would be induced as a result of the ascent of the mafic end-member of the low-K products of the first stage. This magma would be still active also in the second stage (Fig. 8). The mafic magma from deeper levels is characterized by high-Cr type. This type mafic magma differentiate into low-Cr type through the AFC process as described for the formation of the low-Cr mafic magmas of stages 1 and 3 by Hirotani et al. (2009). The low-Cr type mafic magma would ascent further. When the mafic magma reached shallow crustal level where the remnant of stage 1 medium-K felsic magma chamber locates, the mafic magma would re-activate this felsic chamber by its heat. The higher Zr, Hf, U, and Th contents of the felsic end-member magma can be explained by the melting of the accessory zircon minerals with thorite inclusions during the re-activation. The re-activated felsic magma would mix with the low-Cr type mafic magma in the chamber. The schematic representation of the magma feeding system is presented in Fig. 8.

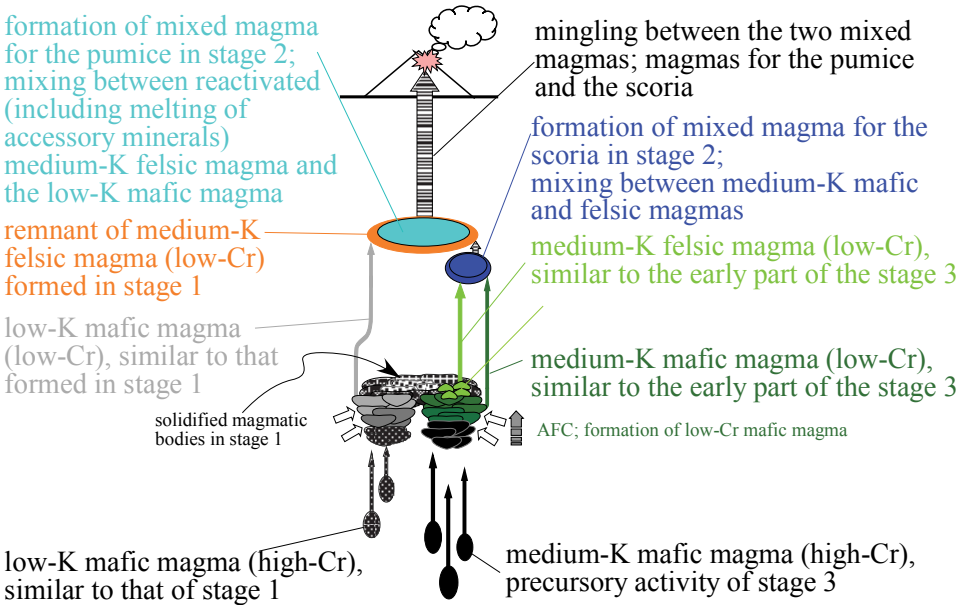

Fig. 8. Schematic representation of the magma feeding system of the stage 2 in the Shirataka volcano.

5.3.2 Formation of mixed magma for the scoria

The third stage mafic end-member magma would antecedently appear as the mafic end-member for scoria at the second stage. The felsic end-member magma for the scoria was generated by the melt extraction or re-melting process, and subsequently mixed with the mafic end-member in a crustal magma chamber. The Mg# and the estimated precipitated temperature of two-pyroxenes in the scoria are higher than those in the other felsic end-members (Hirotani & Ban, 2006). Furthermore the size of the pyroxene phenocrysts is smaller than those in the other felsic end-members, but larger than the groundmass minerals. These features indicate that the pyroxenes of the scoria are grouped to group III (population III of Hirotani et al. (2009)), and precipitated from the mixed magma for the scoria in the chamber, suggesting that the mixed magma was stored in the crust for a while.

5.3.3 Mingling between two mixed magmas

Consequently, two kinds of mixed magma were stored at shallow crust level. One is for the pumice and the other is for the scoria. Further ascent of the mafic end-member triggered the ascent of the mixed magma of the scoria. This mixed magma would tap the shallow chamber filled with the other mixed magma of the pumice. Finally, these two mixed magmas erupted synchronously, which made the eruption explosive. In addition, rarely observed banded pumice would be formed probably during the ascent through the conduit.

6. Conclusions

Detailed petrologic study on the explosive pyroclastic eruption stage of the Shirataka volcano, NE Japan, produced the following results. The eruptive products are mostly pumice with minor amount of scoria. Banded pumice is rarely observed.

1. Both the pumice and scoria were formed by two end-members mixing. The estimated end-member components for the pumice are similar to those activated in the first stage. Whereas, those for the scoria are similar to those of the third stage.
2. The felsic end-member magma for the pumice shows extremely high Zr, Hf, Th, and U contents than felsic magmas in the other stages. These high contents can be explained by the melting of accessory zircon crystals, which have thorite inclusions, when the felsic magma was formed by the re-activation of previously stalled felsic chamber.
3. The hybrid magmas for the pumice and scoria were formed in the crustal chambers before the explosive eruption. During the synchronized eruption, the mixing/mingling between the two magmas occurred, resulting in the formation of the banded pumice.
4. The second stage was transitional one from the first to the third, and the mafic magmas of the first and third stages were simultaneously ascended to the shallow magma feeding system. The former re-activated the felsic magma chamber formed in the first stage, while the latter is regarded as the antecedent activity of the third stage. Finally, there was the ascent of the mixed magma from depth that subsequently tapped the shallow chamber filled with the other mixed magma, which caused the explosive eruption.

7. Acknowledgment

We greatly appreciate anonymous reviewer for many constructive review comments on the early version of the manuscript. The manuscript was greatly improved by the comments. We are grateful for Dr. S. Nakano for supporting this study. We also thank K. Yamanobe for assisting with the ICP-MS measurements.

8. References

Bacon, C. R. (1986) Magmatic inclusions in silicic and intermediate volcanic rocks. *J. Geophys. Res,* 91, 6091-6112.

Ban, M., Hirotani, S., Wako, A., Suga, T., Iai, Y., Kagashima, S., Shuto, K. & Kagami, H. (2007). Origin of silicic magmas in a large-caldera-related stratovolcano in the central part of NE Japan - Petrogenesis of the Takamatsu volcano -. *J. Volcanol. Geotherm. Res.,* 167, 100-118.

Eichelberger, J. C. (1980) Vesiculation of mafic magma during replenishment of silicic magma reservoirs. *Nature*, 288, 446-450.

Feeley, T. C., Dungan, M. A. & Frey, F. A. (1998) Geochemical constraints on the origin of mafic and silicic magmas at Cordon El Guadal, Tatara-San Pedro Complex, central Chile. *Contrib. Mineral. Petrol.,* 131, 393-411.

Gill, J. B. (1981) *Orogenic andesites and plate tectonics,* Springer-Verlag, Berlin. pp 385.

Girard, G. & Stix, J. (2009) Magma recharge and crystal mush rejuvenation associated with early post-collapse upper basin member rhyolites, Yellowstone Caldera, Wyoming. *J. Petrol.,* 50, 2095-2125.

Hansen, J., Skjerlie, K. P., Pederson, R. B. & Rosa, J. D. L. (2002) Crustal melting in the lower parts of island arcs: an example from the Bremanger Granitoid Complex, west Norwegian Caledonides. *Contrib. Mineral. Petrol.,* 143, 316-335.

Hirotani, S. & Ban, M. (2006) Origin of silicic magma and magma feeding system of Shirataka volcano, NE Japan. *J. Volcanol. Geotherm. Res.,* 156, 229-251.

Hirotani, S., Ban, M. & Nakagawa, M. (2009) Petrogenesis of mafic and associated silicic end-member magmas for calc-alkaline mixed rocks in the Shirataka volcano, NE Japan. *Contrib. Mineral. Petrol.,* 157, 709-734.

Huber, C., Bachmann, O. & Dufek, J. (2010) The limitations of melting on the reactivation of silicic mushes. *J. Volcanol. Geotherm. Res.,* 195, 97-105.

Ishii, M. & Saito, K. (1997) A K-Ar age study on Shirataka volcano, Yamagata Prefecture. *Bull. Yamagata Univ., Nat. Sci.*, 14, 99-108.

Ishizuka, O., Yuasa, M., Tamura, Y., Shukuno, H., Stern, R. J., Naka, J., Joshima, M. & Taylor, R. N. (2010) Migrating shoshonitic magmatism tracks Izu–Bonin–Mariana intra-oceanic arc rift propagation. *Earth Planet. Sci. Lett.,* 294, 111–122.

Kawano, Y., Yagi, K. & Aoki, K. (1961) Petrography and petrochemistry of the volcanic rocks of Quaternary volcanoes of northeastern Japan. *Sci. Rep. Tohoku Univ. Ser III,* 7, 1-46.

Mimura, K. & Kanno, K. (2000) Stratigraphy and history of Shirataka volcano, NE Japan. *Bull. Volcanol. Soc. Jpn.*, 45, 13-23.

McCurry, M. & Rodgers, D. W. (2009) Mass transfer along the Yellowstone hotspot track I: petrologic constraints on the volume of mantle-derived magma. *J. Volcanol. Geotherm. Res.,* 188, 86-98.

Nakagawa, M., Shimotori, H. & Yoshida, T. (1988) Across-arc compositional variation of the Quaternary basaltic rocks from the Northeast Japan arc. *J. Mineral. Petrol. Econ. Geol.,* 83, 9-25.

Nakagawa, M., Kitagawa, J. & Furukawa, R. (2003) Sequential caldera-forming eruptions from multiple magma chambers of Shikotsu caldera, Hokkaido, Japan. *XXIII General Assembly of the International Union of Geodesy and Geophysics,* Abstract V08/02P/A02-005.

Paquett, J. L. & Mergoil-Daniel, J. (2009) Origin and U–Pb dating of zircon-bearing nepheline syenite xenoliths preserved in basaltic tephra (Massif Central, France). *Contrib. Mineral. Petrol.,* 158, 245–262.

Rowe, M. C., Wolff, J. A., Gardner, J. N., Ramos, F. C., Teasdale, R. & Heikoop, C. E. (2007) Development of a continental volcanic field: petrogenesis of pre-caldera intermediate and silicic rocks and origin of the Bandelier magmas, Jemez Mountains (New Mexico, USA). *J. Petrol.,* 48, 2063-2091.

Rubatto, D. & Hermann, J. (2007) Experimental zircon/melt and zircon/garnet trace element partitioning and implications for the geochronology of crustal rocks. *Chem. Geol.*, 241, 38–61.

Sakuyama, M. (1981) Petrological study of the Myoko and Kurohime volcanoes, Japan: crystallization sequence and evidence for magma mixing. *J. Petrol.,* 22, 553-583.

Shane, P., Martin, S. B., Smith, V. C., Beggs, K. F., Darragh, Cole, J. W. & Nairn, I. A. (2007) Multiple rhyolite magmas and basalt injection in the 17.7 ka Rerehakaaitu eruption episode from Tarawera volcanic complex, New Zealand. *J. Volcanol. Geotherm. Res.,* 164, 1-26.

Smith, I. S. E., Worthington, T. J., Price, R. C., Stewart, R. B. & Maas, R. (2006) Petrogenesis of dacite in an oceanic subduction environment: Raoul Island, Kermadec arc. *J. Volcanol. Geotherm. Res.,* 156, 252-265.

Tamura, Y. & Tatsumi, Y. (2002) Remelting of an andesitic crust as a possible origin for rhyolitic magma in oceanic arcs: an example from the Izu-Bonin arc. *J. Petrol.*, 43, 1029-1047.

Tatsumi, Y. & Eggins, S. (1995) *Subduction zone magmatism*, Blackwell: Oxford, pp 211.

Tsuchiyama, A. (1985) Dissolution kinetics of plagioclase in the melt of the system diopside-albite-anorthite, and origin of dusty plagioclase in andesites. *Contrib. Mineral. Petrol.*, 89, 1-16.

Wolff, J. A., Wark, D. A., Ramos, F. C. & Olin, P. H. (2006) Petrologic evidence for thermal rejuvenation of crystal mush in the Bandelier Tuff. *Eos Trans. AGU, 87(52), Fall Meet. Suppl.,* Abstract V24C-01.

Vogel, T. A., Patino. L. C., Jonathon K. Eaton, J. K., Valley, J. W., Rose, W. I., Alvarado, G. E. & Viray, E. L. (2006) Origin of silicic magmas along the central American volcanic front: Genetic relationship to mafic melts. *J. Volcanol. Geotherm. Res.,* 156, 217-228.

Yagi, H., Soda, T, Inokuchi, T., Haraguchi, T. & Ban, M. (2005) Catastrophic collapse of Mt. Zao and Mt. Shirataka and their chronological timing. *The Quaternay Res.,* 44, 263-272.

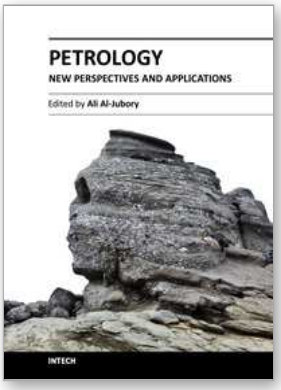

Petrology - New Perspectives and Applications
Edited by Prof. Ali Al-Juboury

ISBN 978-953-307-800-7
Hard cover, 224 pages
Publisher InTech
Published online 13, January, 2012
Published in print edition January, 2012

Petrology, New Perspectives and Applications is designed for advanced graduate courses and professionals in petrology. The book includes eight chapters that are focused on the recent advances and application of modern petrologic and geochemical methods for the understanding of igneous, metamorphic and even sedimentary rocks. Research studies contained in this volume provide an overview of application of modern petrologic techniques to rocks of diverse origins. They reflect a wide variety of settings (from South America to the Far East, and from Africa to Central Asia) as well as ages ranging from late Precambrian to late Cenozoic, with several on Mesozoic/Cenozoic volcanism.

InTech Europe
University Campus STeP Ri
Slavka Krautzeka 83/A
51000 Rijeka, Croatia
Phone: +385 (51) 770 447
Fax: +385 (51) 686 166
www.intechopen.com

InTech China
Unit 405, Office Block, Hotel Equatorial Shanghai
No.65, Yan An Road (West), Shanghai, 200040, China
中国上海市延安西路65号上海国际贵都大饭店办公楼405单元
Phone: +86-21-62489820
Fax: +86-21-62489821